



THE UNIVERSITY *of* EDINBURGH

Edinburgh Research Explorer

Communication: Heavy Rydberg states: The H+H- system

Citation for published version:

Kirrandar, A 2010, 'Communication: Heavy Rydberg states: The H+H- system' Journal of Chemical Physics, vol 133, no. 12, 121103, pp. -, 10.1063/1.3492371

Digital Object Identifier (DOI):

[10.1063/1.3492371](https://doi.org/10.1063/1.3492371)

Link:

[Link to publication record in Edinburgh Research Explorer](#)

Document Version:

Publisher final version (usually the publisher pdf)

Published In:

Journal of Chemical Physics

Publisher Rights Statement:

Copyright 2010 by the American Institute of Physics. This article may be downloaded for personal use only. Any other use requires prior permission of the author(s) and the American Institute of Physics.

General rights

Copyright for the publications made accessible via the Edinburgh Research Explorer is retained by the author(s) and / or other copyright owners and it is a condition of accessing these publications that users recognise and abide by the legal requirements associated with these rights.

Take down policy

The University of Edinburgh has made every reasonable effort to ensure that Edinburgh Research Explorer content complies with UK legislation. If you believe that the public display of this file breaches copyright please contact openaccess@ed.ac.uk providing details, and we will remove access to the work immediately and investigate your claim.



Communication: Heavy Rydberg states: The $H+H^-$ system

Adam Kirrander

Citation: *J. Chem. Phys.* **133**, 121103 (2010); doi: 10.1063/1.3492371

View online: <http://dx.doi.org/10.1063/1.3492371>

View Table of Contents: <http://jcp.aip.org/resource/1/JCPSA6/v133/i12>

Published by the [AIP Publishing LLC](#).

Additional information on *J. Chem. Phys.*

Journal Homepage: <http://jcp.aip.org/>

Journal Information: http://jcp.aip.org/about/about_the_journal

Top downloads: http://jcp.aip.org/features/most_downloaded

Information for Authors: <http://jcp.aip.org/authors>

ADVERTISEMENT



Explore the **Most Cited**
Collection in Applied Physics

AIP
Publishing

Communication: Heavy Rydberg states: The H^+H^- system

Adam Kirrander^{a)}

Laboratoire Aimé Cotton du CNRS, Université de Paris-Sud, 91405 Orsay, France

(Received 10 August 2010; accepted 31 August 2010; published online 30 September 2010)

Heavy Rydberg states are analogs of electronic Rydberg states, but with the electron replaced by a much heavier ion. We calculate *ab initio* the extremely long-range vibrational H^+H^- heavy Rydberg states in H_2 , and compare these to recent experiments. The calculated resonance positions and widths agree well with experiment, but we predict additional sharp interloper resonances corresponding to vibrational states trapped inside the barrier on potential energy curve $7\ ^1\Sigma_g^+$.

© 2010 American Institute of Physics. [doi:10.1063/1.3492371]

Rydberg states, characterized by long range Coulomb interactions, normally between an electron and a positively charged atomic or molecular ion or even a positron, also occur in ionic bonds between atoms. In a series of recent experiments, Vieitez *et al.*^{1,2} observed H^+H^- vibrational heavy Rydberg states in photoexcited H_2 . These exotic states exhibit extremely large amplitude vibrations and can be regarded as molecular analogs of excited electronic states of alkali atoms, but with a positively charged proton orbiting a negative closed shell ion, $\text{H}^-(1s^2)$. Nonadiabatic couplings in the H^+H^- collision complex lead to electron transfer and subsequent dissociation into neutral atomic fragments. This mutual neutralization affects the astrophysically important H_2 formation rate.³ More generally, molecular ion-pair states participate in the dissociative photodynamics of a wide range of molecules and appear in the context of threshold ion-pair product spectroscopy.⁴

In this Communication, we calculate *ab initio* the dynamics of the heavy Rydberg states observed by Vieitez *et al.* We confirm the experimental conclusion² that the lifetimes do not follow the established n_{IP}^{-3} scaling law for Rydberg states and trace the cause to the large difference in reduced mass between electronic and heavy Rydberg states. The large mass of the latter leads to greater spacing of energy levels and hence greater variation in the short range interactions, meaning that much higher principal quantum numbers n_{IP} are required before the n_{IP}^{-3} scaling law is valid. In H_2 , we suggest a Landau-Zener type mechanism, where coupling to dissociation decreases with increasing energy, as partial explanation to the long lifetimes observed for $n_{IP} \geq 2000$ states.⁵ Finally, our calculations predict not yet observed, inside-the-barrier resonances on potential energy curve $7\ ^1\Sigma_g^+$, which could well exist in many molecules.⁶ Overall, the agreement between experiment and theory is good.

Our first-principles quantum mechanical calculation uses available *ab initio* potential energy curves and nonadiabatic couplings. The close-coupled equations for nuclear motion on the potential energy curves are integrated using the log derivative method.⁷ For heavy Rydberg states with high principal quantum number this is combined with the highly ac-

curate elimination of long-range closed channels by generalized multichannel quantum defect theory (MQDT).^{8,9} Essentially the nuclear dynamics is considered to take place in two regions, depending on the internuclear coordinate R , separated by the matching radius R_f and the classical turning point for the heavy Rydberg state, R_{IP} . In the inner region, $0 < R < R_f$, the strong nonadiabatic coupling leads to electron transfer and dissociation into neutral atoms, $\text{H}(1s) + \text{H}(n=2-4)$. In the outer region, $R_f < R < R_{IP}$, couplings between channels are absent, but the ion-pair channel gives rise to long-range resonances. Asymptotically, for $R > R_{IP}$, only dissociated neutral atoms persist. For $n_{IP}=2000$, $R_f=350$ and $R_{IP}=8710$ a.u., as shown in Fig. 1.

The calculated resonances are assigned a principal quantum number, n_{IP} , and a quantum defect, μ , by reference to the Rydberg formula,

$$\frac{E_n}{hc} = D_{\text{H}^+\text{H}^-} - \frac{Ry_\infty(M/m_e)}{(n_{IP} - \mu)^2}, \quad (1)$$

where Ry_∞ is the infinite-mass Rydberg constant, $(M/m_e) = 918.5761$ is a mass-scaling factor with M the reduced mass of H^- and m_e the mass of an electron, and $D_{\text{H}^+\text{H}^-} = 139\,713.83\ \text{cm}^{-1}$ ($-0.527\,751\,014$ a.u.)^{2,10} is the ion-pair dissociation energy. The quantum defect, μ , gives the shift in the heavy Rydberg state position compared to a pure Coulomb state. The shift is caused by nonadiabatic couplings and the non-Coulombic nature of the potentials at short range, and also, in some smaller part by the long-range polarizability of the ion-pair potential. The ion-pair potential¹¹ shown in Fig. 1 is given by

$$E^{\text{ion}}(R) = D_{\text{H}^+\text{H}^-} - \frac{1}{R} - \frac{\alpha_{\text{H}^-}}{2R^4}, \quad (2)$$

in atomic units, where the polarizability of $\text{H}^-(1s^2)$ is $\alpha_{\text{H}^-} = 211.897$ a.u.^{3,12}

We solve the close-coupled equations for nonadiabatic nuclear motion in the standard form, obtained by a Cayley transform of the nonadiabatic equations,

^{a)}Electronic mail: adam.kirrander@gmail.com.

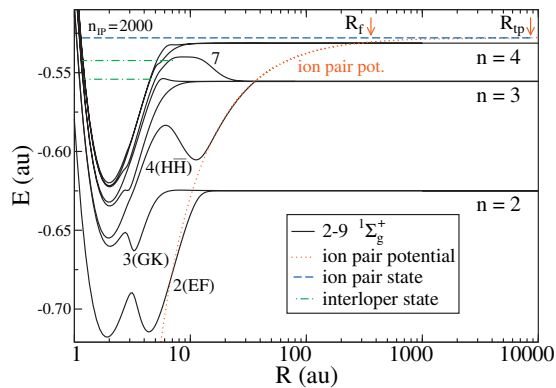


FIG. 1. *Ab initio* potential energy curves 2–9 $^1\Sigma_g^+$ for H_2 (Refs. 11, 13, and 14). The dotted line is the ion-pair potential [see Eq. (2)]. The sharp interloper resonances around $n_{IP}=130$ and 190 (see Table I) trapped inside the repulsive barrier on 7 $^1\Sigma_g^+$ are indicated with horizontal lines, as is the $n_{IP}=2000$ heavy Rydberg state, with corresponding matching radius $R_f=350$ a.u. and classical turning point $R_{IP}=8710$ a.u. indicated by arrows. Potential energy curves EF, GK, HH and 7 are labelled.

$$\Psi''(R) = W(R)\Psi(R), \quad (3)$$

where Ψ is a $N' \times N'$ matrix, each column a linearly independent solution, Ψ'' indicates the second derivative with respect to R and the matrix W consists of

$$W(R) = \frac{2M}{\hbar^2} V(R) - k^2, \quad (4)$$

where the $N' \times N'$ matrix V contains the diagonal potentials and the off-diagonal coupling elements. The diagonal matrix k contains the asymptotic channel wave vectors $k^2 = (2M/\hbar^2)\epsilon$, where ϵ has diagonal elements $\epsilon_i = E - E_i$, with E the total energy and E_i the threshold energy in each channel i . The *ab initio* potential energy curves and the nonadiabatic couplings are taken from Wolniewicz *et al.*^{11,13} for states 2–6 $^1\Sigma_g^+$, and from Cederbaum *et al.*¹⁴ for states 7–9 $^1\Sigma_g^+$. The potentials are shown in Fig. 1. The weakly avoided crossings between the ion-pair potential and the adiabatic potential energy curves at $R \approx 36$ a.u. ($n=3$) and $R \approx 280$ a.u. ($n=4$) are fitted. Overall, the nonadiabatic couplings are particularly strong for $R < 20$ a.u..

Equation (3) is solved using the log derivative method,⁷ which propagates the log derivative matrix $Y(R) = \Psi'(R)\Psi^{-1}(R)$ instead of propagating the wave function Ψ directly. The matrix is propagated out to the matching radius R_f , where it is used to calculate the wave function in the form $\Psi = F - GK$, where F and G are diagonal $N \times N$ matrices containing energy normalized Milne functions.¹⁵ These coincide with analytic Coulomb and Riccati–Bessel functions when the polarization term in Eq. (2) vanishes. Note that $N \leq N'$, since channels closed already at R_f are excluded from Ψ . The crucial entity is the $N \times N$ reaction matrix K , which summarizes all interactions for $R < R_f$, and that is used in the remainder of the calculation.

The next step deals with the outer region where the heavy Rydberg wave functions extend to large distances and give rise to sharp long-range resonances in the ion-pair channel. We eliminate the asymptotically closed ion-pair channel analytically. The elimination procedure uses the $N = N_o + N_c$

(open+closed) linearly independent solutions at R_f given by the column vectors of the wave function Ψ to form N_o superposition wave functions Φ ($N \times N_o$ matrix) with correct asymptotic boundary conditions. The superposition wave function can be written as $\Phi = \Psi Z = (FC - GS)B$, where Z is the $N \times N_o$ superposition coefficient matrix and for the second equality we use $Z = CB$, defining the $N \times N$ matrices S and C such that $K = SC^{-1}$. Following the well-established procedures of MQDT,⁸ solutions with correct asymptotic boundary conditions can be found by solving the generalized eigenvalue equation,

$$\Gamma B = \tan \pi \tau_\rho \Lambda B, \quad (5)$$

whereby we determine the N_o eigenphases $\pi \tau_\rho$ and the $N \times N_o$ coefficient matrix B . The $N \times N$ matrices Γ and Λ are defined as

$$\begin{aligned} \Gamma_{ii'} &= \sin \beta_i C_{ii'} + \cos \beta_i S_{ii'}, & i \in \text{closed} \\ \Lambda_{ii'} &= 0, & i \in \text{closed} \\ \Gamma_{ii'} &= S_{ii'}, & i \in \text{open} \\ \Lambda_{ii'} &= C_{ii'}, & i \in \text{open}, \end{aligned} \quad (6)$$

where $\beta_i(\epsilon_i)$ is the accumulated phase in the closed ion-pair channel.

Finally, it is straightforward to calculate the asymptotic open-open ($N_o \times N_o$) energy-dependent scattering matrix $S^-(E)$, corresponding to the incoming wave boundary conditions appropriate for photodissociation half-collisions,

$$S_{ij}^- = e^{-i\gamma_i} \sum_{\rho=1}^{N_o} T_{i\rho} e^{-i2\pi\tau_\rho} T_{\rho j}^{-1} e^{-i\gamma_j}, \quad (7)$$

where γ_i is the asymptotic phase in channel i and the unitary matrix T is defined by $T = CB \cos \pi \tau + SB \sin \pi \tau$. The density of states is calculated from the derivative of the cumulative eigenphase, $d(\sum_\rho \pi \tau_\rho(E))/dE$.

In the experiments of Vieitez *et al.*,² excitation is either via a $J'=0$ intermediate state, leading to a Rydberg series with total angular momentum $J=1$ or via a $J'=1$ state, leading to $J=0$ and 2 series. In the $J=0,2$ experiments, only one Rydberg series is observed. From our calculations for $n_{IP}=130-230$ shown in Fig. 2, it is evident that the energy splitting between the two series is too small to be resolved in the experiments.

In all three calculated $J=0-2$ series, the heavy Rydberg states shift smoothly as a function of J , and sharp non-Rydberg interlopers appear around $n_{IP}=130$ and $n_{IP}=190$. These resonances, listed in Table I, correspond to states trapped inside the broad repulsive barrier on 7 $^1\Sigma_g^+$ around $R=7-12$ a.u. (see Fig. 1), which is due to electronic interaction between atom and Rydberg atom in the collision complex,⁶ in a mechanism analogous to the one proposed for the formation of ultra-long-range Rydberg molecules¹⁶ in ultracold dense gases. Barriers such as the barrier on 7 $^1\Sigma_g^+$ are a general occurrence in diatomic molecules,⁶ and therefore similarly trapped vibrational states could be expected in other molecules. In H_2 , the barrier appears in the Σ manifold, and is particularly prominent in the $^1\Sigma_g^+$ and $^1\Sigma_u^+$ symmetries, which both support H^+H^- heavy Rydberg states. Since these sharp inside-the-barrier resonances are confined to small in-

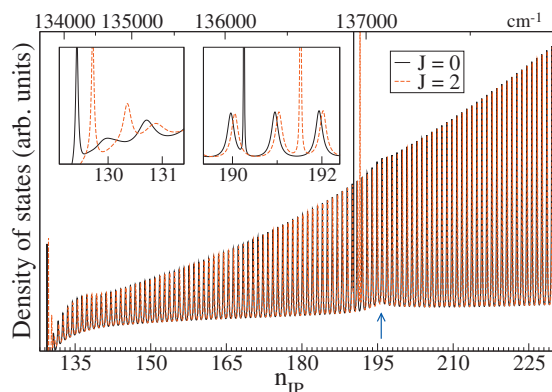


FIG. 2. The calculated resonances (density of states) for $\text{H}_2(^1\Sigma_g^+)$ $J=0,2$ plotted as a function of principal quantum number n_{IP} (spectroscopic energies relative to the H_2 ground state in cm^{-1} along upper x-axis). The two insets show the interloper resonances at $n_{IP} \approx 130$ and $n_{IP} \approx 190$ more clearly. The arrow marks the change in background phase above the potential barrier on $7^1\Sigma_g^+$ (see text).

ternuclear distances, they are more sensitive to the value of J than the heavy Rydberg states, and strong coupling to ionization is expected. Note finally the pronounced change in the background phase for energies just above the barrier, marked by an arrow in Fig. 2.

The positions of the resonances are analyzed in terms of the quantum defect assigned to each resonance, which gives the shift compared to a pure Coulomb state. In Fig. 3, the quantum defects μ are given as a function of the principal quantum number n_{IP} for the series $J=0-2$ and compared to experimental measurements by Vieitez *et al.*² Overall, we see good agreement. Note that the energy dependence is almost linear. Also included in Fig. 3 are quantum defects calculated from a simple diabatic model that uses a constructed $\text{H}\bar{\text{H}} \rightarrow \text{H}^+\text{H}^-$ potential curve to calculate the $J=0$ series for $n_{IP} = 160-230$. This gives quite good agreement, indicating that the heavy Rydberg dynamics is dominated by the $\text{H}\bar{\text{H}}$ potential at short internuclear distances.

The calculated widths in Fig. 4 are narrower than the experimental observations, but within one σ -error of the fitted experimental data.² The existing discrepancies can most likely be attributed to coupling to ionization, which is known to be significant.^{1,2} It is possible, for instance, that the jump in quantum defects and widths in the experimental data at $n_{IP} \approx 160$, see Figs. 3 and 4, is due to an electronic Rydberg resonance. The calculated widths do not follow the estab-

TABLE I. Inside-the-barrier interloper resonances for $J=0-2$, including the energy relative to the H_2 ground state, effective quantum number, ($\nu_{IP} = n_{IP} - \mu$), and full width at half maximum.

| J | E (cm^{-1}) | ν_{IP} | Width (cm^{-1}) |
|-----|---------------------------|------------|-------------------------------|
| 0 | 133 696 | 129.42 | 5.644 |
| | 136 929 | 190.26 | 0.215 |
| 1 | 133 707 | 129.55 | 1.608 |
| | 136 941 | 190.69 | 0.336 |
| 2 | 133 723 | 129.72 | 6.407 |
| | 136 966 | 191.52 | 0.746 |

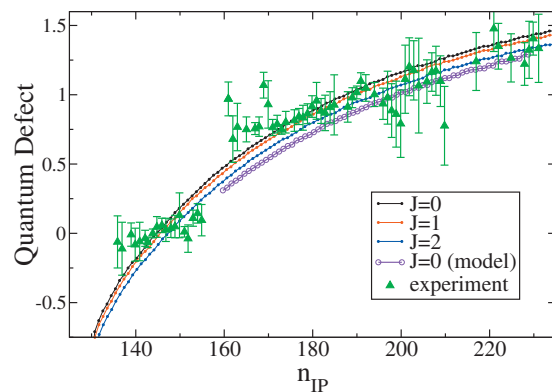


FIG. 3. Quantum defects as a function of principal quantum number n_{IP} for $J=0-2$. The sharp interloper resonances in Table I are not included. Experimental data from Vieitez *et al.* (Refs. 1 and 2). The calculated data for the $J=0$ (model) correspond to dynamics on a single diabatic potential (see text).

lished n_{IP}^{-3} scaling law for Rydberg states,¹⁷ even when the very narrow interloper resonances are excluded. On the contrary, for $n_{IP}=136-141$ the widths increase, while for $n_{IP} > 141$ the widths decrease more rapidly than n_{IP}^{-3} . In previous experiments, Reinhold and Ubachs⁵ observed wave packets formed from H^+H^- heavy Rydberg states with principal quantum number $n_{IP} \geq 2000$, finding lifetimes close to 90 ns, two orders of magnitude longer than expected² based on n_{IP}^{-3} extrapolation of the widths at $n_{IP} \approx 200$. This was attributed to J -mixing by external fields, analogous to the ℓ -mixing in electronic zero electron kinetic energy (ZEKE) spectroscopy.⁵ In our calculations, we find that the line widths for $n_{IP}=2000$ are $5 \times 10^{-4} \text{ cm}^{-1}$, corresponding to lifetimes around 10 ns, already much closer to the experimental observations, suggesting that the effect of J -mixing is less dramatic than previously assumed.

The origin of the apparent failure of the n_{IP}^{-3} scaling law is the great difference in reduced mass between a negative ion and an electron. Consequently, while the energy levels of the electron occupy a narrow band just below the ionization limit, the levels of the heavy Rydberg system span a wider energy range. Only once the short range interactions, or equivalently the reaction matrix \mathbf{K} , become independent of the principal quantum number ($n_{IP} \geq 500$ in H^+H^-) is the n_{IP}^{-3}

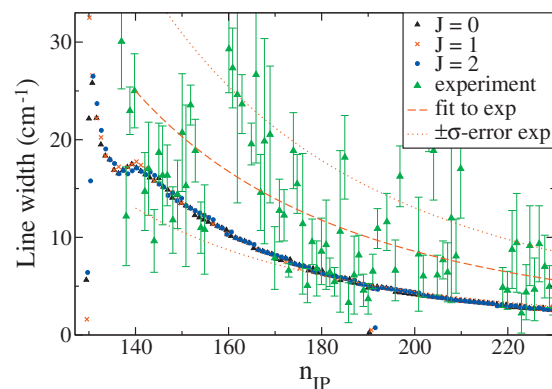


FIG. 4. Line widths in cm^{-1} as a function of principal quantum number n_{IP} for $J=0-2$. Least-square fits $\Gamma \propto n_{IP}^{-3}$ to the experimental data (Refs. 1 and 2) (dashed line) together with $\pm\sigma$ -error (dotted lines).

scaling law recouped. For instance, in our calculations in the region of $n_{IP} \approx 2000$, the n_{IP}^{-3} scaling law is valid and the quantum defects are essentially constant. In H_2 , the n_{IP} -dependence of the K -matrix leads to increasingly narrow lines, possibly by a Landau–Zener type mechanism that results in reduced coupling to dissociation at higher energies as the interactions in the H^+H^- collision complex become increasingly diabatic.

In summary, we have combined generalized MQDT and the log derivative method. The method is applied to recent observations of photoexcited H_2 by Vieitez *et al.*^{1,2} and the calculations provide a step toward elucidating the molecular dynamics behind the observed heavy Rydberg spectra. The calculated line positions and widths agree with experiments, and a simple calculation using a single diabatic state indicates that the heavy Rydberg dynamics is dominated by the $HH^- \ ^1\Sigma_g^+$ potential at short range. We also find that the predicted energy splitting between the $J=0$ and 2 series is below the experimental resolution, explaining why only one series is observed in experiments via a $J'=1$ intermediate state.² In our calculations, we see evidence for vibrational states trapped inside the barrier on $7 \ ^1\Sigma_g^+$. These, as yet not observed very sharp resonances, should couple strongly to ionization, and could occur in a wide range of diatomic molecules.⁶ For the highly excited $n_{IP} \approx 2000$ heavy Rydberg states, the widths are an order of magnitude narrower than predicted by n_{IP}^{-3} scaling laws, in qualitative agreement with experimental findings.

Given the agreement between observed and calculated line widths and positions, it seems likely that the ionization

continuum does not cause major shifts in the heavy Rydberg spectrum, but it should be noted that the present calculations do not include rotational coupling, coupling to ionization, nor provide actual intensities for the spectra. Work is underway to include these effects, which requires the extension of the present approach at short internuclear distances.

The author gratefully acknowledges helpful discussions with Dr. Christian Jungen and Professor Wim Ubachs. This work was supported by the European Union through a Marie Curie Fellowship (FP7-IEF).

¹M. O. Vieitez, T. I. Ivanov, E. Reinhold, C. A. de Lange, and W. Ubachs, *Phys. Rev. Lett.* **101**, 163001 (2008).

²M. O. Vieitez, T. I. Ivanov, E. Reinhold, C. A. de Lange, and W. Ubachs, *J. Phys. Chem. A* **113**, 13237 (2009).

³S. C. Glover, D. W. Savin, and A.-K. Jappsen, *Astrophys. J.* **640**, 553 (2006).

⁴A. Suits and J. W. Hepburn, *Annu. Rev. Phys. Chem.* **57**, 431 (2006).

⁵E. Reinhold and W. Ubachs, *Phys. Rev. Lett.* **88**, 013001 (2002).

⁶A. S. Dickinson and F. X. Gadea, *Phys. Rev. A* **65**, 052506 (2002).

⁷D. E. Manolopoulos, *J. Chem. Phys.* **85**, 6425 (1986).

⁸C. H. Greene and Ch. Jungen, *Adv. At. Mol. Phys.* **21**, 51 (1985).

⁹F. H. Mies, *J. Chem. Phys.* **80**, 2514 (1984).

¹⁰C. L. Pekeris, *Phys. Rev.* **126**, 1470 (1962).

¹¹L. Wolniewicz, *J. Chem. Phys.* **108**, 1499 (1998).

¹²A. Dalgarno, *Adv. Phys.* **11**, 281 (1962).

¹³L. Wolniewicz and K. Dressler, *J. Chem. Phys.* **100**, 444 (1994).

¹⁴T. Detmer, P. Schmelcher, and L. S. Cederbaum, *J. Chem. Phys.* **109**, 9694 (1998).

¹⁵Ch. Jungen and F. Texier, *J. Phys. B* **33**, 2495 (2000).

¹⁶C. H. Greene, A. S. Dickinson, and H. R. Sadeghpour, *Phys. Rev. Lett.* **85**, 2458 (2000).

¹⁷T. F. Gallagher, *Rydberg Atoms*, 1st ed. (Cambridge University Press, Cambridge, 1994).